

# CORRELATION EFFECTS OF FREQUENCY HOPPING DIVERSITY SYSTEMS IN INDOOR MOBILE COMMUNICATIONS ENVIRONMENTS

R.AGUSTI and P.DIAZ  
Department of Signal Theory and Communications  
Universitat Politècnica de Catalunya

**Abstract-** Frequency-Hopping (FH) techniques in conjunction with coding have been proposed for indoor radio systems based on the fact that FH behaves as an intrinsic frequency diversity technique. In this paper we assess the performance of a FH-BPSK for other situations not previously considered in the literature. In particular, the effects of having a non-null correlation coefficient in function of the frequency separation as well as the presence of coding schemes have been considered.

## 1. INTRODUCTION

The performance of an indoor mobile radio system operating in the UHF band is severely affected by the multipath propagation medium. To counteract the effects of the fading one can resort to coding, diversity or combined coding/diversity schemes.

The more recent standard systems of mobile communications use in some extent combined coding/diversity schemes by means of the Frequency Hopping (FH) techniques in order to take advantage of the intrinsic frequency diversity that the FH enable.

In this paper, we analyze the performance of a specifically FH oriented system proposed to be used in indoor communications. In particular, we have analyzed the sensibility of this system with respect to the hopping frequency separation,  $S_r$ .

The mentioned scheme is a TDMA cyclical slow FH system proposed in [1] for indoor applications and similar to the GSM scheme. To take full advantage of its intrinsic frequency diversity, FH has to be used in conjunction with coding and interleaving techniques. In this sense besides the Reed-Solomon (6,2) coding retained in [1] a Repetition coding with the same redundancy has also been introduced. In order to assess the performance of this scheme we have considered a discrete model with a Power Delay Profile modeled as a double Poisson Process [2] that allows us to analyze any transmission rate.

## 2. SIGNALING FORMAT

In order to obtain some representative results of the effects of both the hopping frequency separation and the coding used in the system performance, a signaling format

as proposed in [1] has been retained. For this purpose data packets are formed according to the following steps:

1- Data entering at 64 Kb/s are collected as a 384 bit block 6 ms. long as shown in Table 1.

1	2	3	4	...	384
---	---	---	---	-----	-----

Table 1.

2- A rate 1/3: R-S(6,2) or Repetition code is formed giving a 384 symbol block 6 ns. long.

3- The symbols are stored into a buffer in successive columns and read out in rows as shown in Table 2.

$X_1$	$X_7$	...	$X_{379}$
$X_2$	$X_8$	...	$X_{380}$
$X_3$	$X_9$	...	$X_{381}$
$X_4$	$X_{10}$	...	$X_{382}$
$X_5$	$X_{11}$	...	$X_{383}$
$X_6$	$X_{12}$	...	$X_{384}$

Table 2.

4- Preamble, sync word and spare time are added to each row giving a slot 1 ms. long as shown in Table 3. To make use of the FH intrinsic diversity in the sense that some frequency channels are better than others in terms of the received power and/or distortion, the 6 formed slots are finally modulated according to 6 assigned hopping frequencies.

32	24	192	8
----	----	-----	---

Table 3.

5- The final TDMA FH format results from sharing each 1 ms. frame duration among  $n$  users. The resulting air bit rate is then  $R_B = n \cdot 256$  Kb/s.

## 3. SYSTEM ANALYSIS

Each one of the 6 carriers above mentioned is used to

perform a BPSK modulation. Then, with respect to the transmission point of view, the base band model system is simply formed by a cascade of a transmitter filter, the mobile channel and the receiver filter, so that, the overall impulse response complex envelope in absence of channel distortion is a raised-cosine with a 0.5 Roll-off parameter equally splitted between transmitter and receiver. The complex envelope of the channel impulse response,  $h_N(t)$ , is modeled according to [2] as

$$h(t) = \sum_{l=0}^{\infty} \sum_{k=0}^{\infty} \beta_{k,l} e^{j\theta_{k,l}} \delta(t - \tau_{k,l}) \quad (1)$$

$$\beta_{k,l}^2 = \beta^2(0,0) e^{-\frac{T_l}{\Gamma}} e^{-\frac{\tau_{k,l}}{\rho}}$$

where  $\beta_{k,l}$  and  $\theta_{k,l}$  are Rayleigh and uniformly distributed respectively. Furthermore, in this model the received signal rays arrive in clusters, so that, the arrival times of the rays within the cluster,  $\tau_{k,l}$ , and the clusters themselves,  $T_l$ , are both distributed according two Poisson arrival processes with parameters  $\lambda$  and  $\Delta$  respectively. The model parameters are

$$\Gamma = 60ns, \quad \gamma = 20ns$$

$$\text{Mean Time Between Rays: } \frac{1}{\lambda} = 5ns \quad (2)$$

$$\text{Mean Time Between Clusters: } \frac{1}{\Gamma} = 300ns$$

In the above FH-BPSK system the hopping-frequency separation between the different carriers determine the degree of correlation that the six coded symbols entering the decoder present. Furthermore, the symbol error probability at the input of the decoder is position dependent due to the fact that each group of three bits that make up a symbol is transmitted through a different  $i$ -th frequency channel characterized by a different complex envelope impulse response

$$h_{m,i}(t) = h_m(t) \exp(j2\pi i S_f t) \quad (3)$$

where  $h_m(t)$  is a sample of  $h(t)$ ,  $S_f$  is the hopping-frequency separation and  $i$  varies from 1 to 6.

To obtain the BER at the output of the decoder, the BER at the output of the BPSK detector is first required. For this purpose a combination of analytical and Monte Carlo simulation techniques have been envisaged according to the following two steps procedure:

1. A sample of  $h(t)$ , denoted  $h_m(t)$ , is generated according to its statistical properties. Only rays with amplitudes greater than 0.01 multiplied by the amplitude corresponding to the first ray are taken into account. Considering rays with greater amplitudes they do not change the results significantly.

A squaring timing loop is used for clock recovery.

The sampling instant is [3]

$$t_d = \frac{T}{2\pi} \tan^{-1} \frac{F_{lc}}{F_{rc}} \quad (4)$$

$$F_{rc} + jF_{lc} = \int |h_{m,i}(t) * h_N(t)|^2 dt$$

A loop that eliminates the cross-talk is adopted for carrier recovery. Then [4]

$$\Phi = -\text{Arg } f(t_d) \quad (5)$$

$$f(t) = h_{m,i}(t) * h_N(t)$$

A fast bit error rate, denoted here  $p_{b,m,i}$ , computation method is then used for each  $i$ -th frequency channel. In the simple case that flat fading had been assumed, that is

$$R_b = \frac{1}{T_b} < \frac{1}{D_s} \quad (6)$$

where  $R_b$  denotes the data bit rate. The bit error rate corresponding to the  $i$ -th frequency channel of the  $m$ -th impulse response sample would then be

$$P_{b,m,i} = \frac{1}{2} \text{erfc} \left( \sqrt{\frac{E_{b,m,i}}{N_o}} \right) \quad (7)$$

$$E_{b,m,i} = \frac{1}{2} |H_m(f)|^2 T_b$$

2-The bit error rate,  $p_{b,m}$ , at the decoder output, corresponding to the  $m$ -th sample, is calculated from the symbol error probability at the decoder input given by

$$P_{s,m,i} = 1 - (1 - P_{b,m,i})^3 \quad (8)$$

This is shown in the following for both Reed-Solomon coding and Repetition coding.

### 3.1. REED-SOLOMON CODING

The error probability of the decoded symbols for a given  $h_m(t)$  sample is

$$P_{e,m} = 1 - \prod_{i=1}^6 (1 - P_{s,m,i}) - \sum_{i=1}^6 P_{s,m,i} \prod_{j=1, j \neq i}^6 (1 - P_{s,m,j}) \quad (9)$$

$$- \sum_{i=1}^6 \sum_{k=1, k \neq i}^6 P_{s,m,i} P_{s,m,k} \prod_{l=1, l \neq i, l \neq k}^6 (1 - P_{s,m,l})$$

The  $p_{b,m}$  can be obtained as [5]

$$\frac{1}{2} P_{e,m} \leq P_{b,m} \leq P_{e,m} \quad (10)$$

In order to obtain numerical results, the upper bound of the  $p_{b,m}$  has been retained.

### 3.2. REPETITION CODING

Let the input and the output of the decoder be

Input:  $X_1, X_2$

Output:  $X_1, X_2, X_1, X_2, X_1, X_2$

Then, we have

$$P_{E,m} = P_{s,m,1} P_{s,m,3} (1 - P_{s,m,3}) + P_{s,m,3} P_{s,m,5} (1 - P_{s,m,5}) + P_{s,m,1} P_{s,m,5} (1 - P_{s,m,5}) \quad (11)$$

and the BER can be obtained as

$$P_{b,m} = \frac{1}{2} P_{E,m} \quad (12)$$

3- The final BER results from averaging  $P_{b,m}$  for a great number of  $h_m(t)$  samples.

In the above calculations the signal to noise ratio in the receiver input depends on the  $m$ -th channel impulse response parameters. That is, given the complex envelope of the transmitted signal as

$$s(t) = \sum_n c_n h_T(t - nT) \quad (13)$$

where  $c_n = +1$  or  $-1$  and  $h_T(t)$  is the transmitter impulse response, it can be shown that

$$\frac{E_b}{N_0} = \frac{\lambda \beta^2(0,0) \int_{-\infty}^{\infty} [e^{-\frac{t}{T}} U(t) * h_T^2(t)] dt}{2N_0} \quad (14)$$

where  $E_b$  is the bit energy at the received input and  $U(t)$  is the step function.

The outage probability of great interest in quasi-static indoor environments is also evaluated for the two coding schemes. It is given by

$$\text{Outage Probability} = \text{Prob.}[BER > BER_0] \quad (15)$$

where  $BER_0$  is a threshold bit error rate.

### 4. RESULTS

Some results have been obtained in order to define a proper design value for  $S_f$  as well as to assess the coding system performance of increasing  $R_b$  values, in the presence of both R-S(6,2) and Repetition coding.

At first,  $R_b = 256$  Kb/s has been retained and  $S_f$  values

equal to  $\infty$  MHz., 10 MHz., 5 MHz. and 2.5 MHz. have been considered. The corresponding BER for these cases are displayed in Figures 1,2,3,4 respectively. It can be noticed that no significant variations appear when comparing  $S_f = \infty$  and  $S_f = 10$  MHz. So increasing  $S_f$  beyond 10 MHz. it is not convenient. Another conclusion that could be also extracted from the observation of the Figures 2,3 and 4 is that Reed-Solomon coding outperforms the Repetition coding for  $S_f D_s$  greater than 0.05 approximately.

$R_b$  values of 2.56 Mb/s, 5.12 Mb/s and 10.24 Mb/s have been also considered and similar figures to those shown for the 256Kb/s case have been obtained.  $S_f$  values greater than 10 Mhz are not considered because the changes are not significant. For the observation of the results obtained it can be concluded, for all  $R_b$  values, that Reed-Solomon coding outperforms the Repetition coding for  $S_f D_s$  greater than 0.05 approximately. Whatever  $R_b$  is considered,  $S_f D_s$  greater than about 0.1 and 0.2 for the R-S and Repetition codes respectively does not improve the system performance significantly. This can be better appreciated in Figures 5 and 6 for 256 Kb/s and 5.12 Mb/s respectively. This different behavior of both codes could be explained because the R-S received symbols present a greater correlation than the corresponding repetition symbols involved in the interleaving process. Finally a figure of merit of the system could be given by saying that Outage Rates lower than 0.01 for  $BER = 10^{-3}$  seems possible for  $R_b = 5.12$  Mb/s. In particular, in the case of using Repetition Coding, it is interesting to point out that the receiver could be implemented with low power consumption technologies as needed for realistic portable operation.

### AGREEMENTS

This work has been financed by Spain CICYT TIC880543.

### REFERENCES

- [1] A.A.M. Saleh, A.J.Rustako, Jr., L.J.Cimuni, Jr., "A TDMA indoor radio communications system using cyclical slow frequency hopping and coding-experimental results and implementation issues", Globecom 88.
- [2] A.A.M. Saleh, R.A. Valenzuela, "A statistical model for indoor multipath propagation", IEEE SAC, February 1987.
- [3] J.C-I Chuang, "the effects of multipath delay spread on timing recovery", IEEE Trans. on Vehicular Technology, August 1987.
- [4] S.Moridi, H.Sari, "Analysis of decision-feedback carrier recovery loops with application to 16 QAM digital radio systems", ICC 1983.
- [5] D. Torrieri, "The information bit rate for block codes", IEEE Trans. on Comm., April 1984.

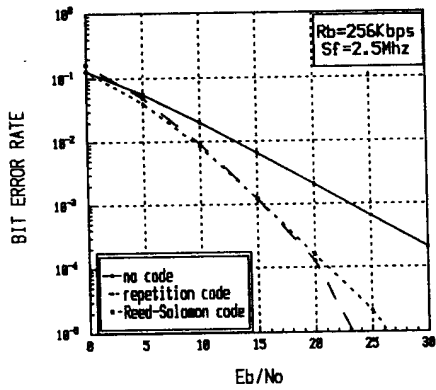


Figure 1. BER for  $R_b=256\text{Kb/s}$  and  $S_f=2.5\text{Mhz}$

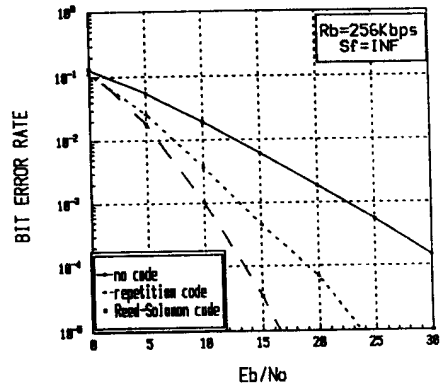


Figure 4. BER for  $R_b=256\text{Kb/s}$  and  $S_f=\text{infinity}$

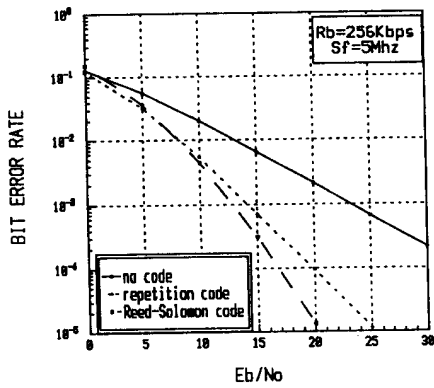


Figure 2. BER for  $R_b=256\text{Kb/s}$  and  $S_f=5\text{Mhz}$

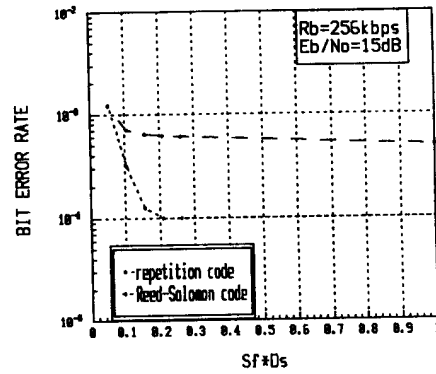


Figure 5. BER versus normalized FH separation for  $R_b=256\text{Kb/s}$

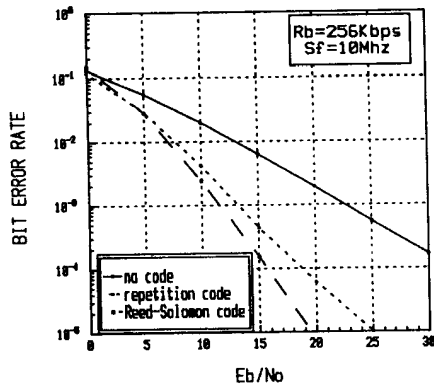


Figure 3. BER for  $R_b=256\text{Kb/s}$  and  $S_f=10\text{Mhz}$

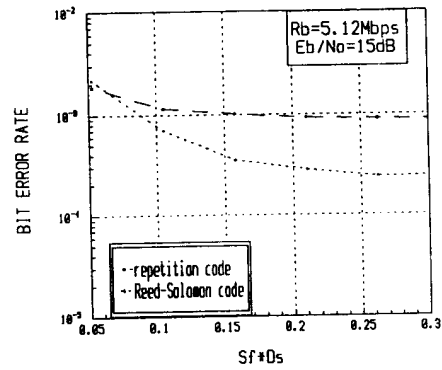


Figure 6. BER versus normalized FH separation for  $R_b=5.12\text{Mb/s}$